Adaptive Friction Compensation: A Globally Stable Approach

K.A.J. Verbert, R. Tóth, *Member, IEEE*. R. Babuška

***Abstract*—In this paper, an adaptive friction compensation scheme is proposed. The friction force is computed as a time-varying friction coefficient multiplied by the sign of the velocity and an on-line update law is designed to estimate this coefficient based on the actual position and velocity errors. Furthermore, a modified signum function definition is proposed to better capture the behavior of friction over varying velocity profiles than the signum function commonly used in friction models. The properties of the closed-loop behavior of the proposed scheme are analyzed and stability of the closed-loop system is proven. Simulations and real-world experimental results are provided to confirm the theoretical findings: the compensator is able to eliminate steady-state errors, significantly decrease the stick-slip effect and compensate even rapidly varying friction forces.**

***Index Terms*—Friction compensation; Adaptive control; Tracking control; Global stability.**

I. Introduction

MANY motion control tasks, like micro-manipulation or robotic surgery, require high precision. In such applications, friction is often the main cause of performance degradation. In the absence of a correct compensatory action, friction may cause significant tracking errors, stick-slip motion and limit cycles [1]. The result is that the controlled system is unable to satisfy high-accuracy performance requirements. Thus, friction compensation is an important objective in motion control. Due to the complexity of the friction phenomenon, it is not easy to adequately compensate for its effects in a closed-loop system. The phenomenon is non-linear (especially in the low-velocity range), time varying and application specific. One way of dealing with friction is to use extra control force to cancel the effect of the friction force [2]. The magnitude of this extra force should be (approximately) equal to the actual friction force. As the friction force is not measurable and it often exhibits unpredictable behavior, its estimation presents a significant challenge. Furthermore, due to the time-varying nature of friction, an a priori estimate/model is often found to be inefficient for compensation. This suggests that adaptive techniques can provide an attractive solution in handling such a complicated time-varying and application-specific behavior.

In the literature, a wide range of adaptive estimation techniques have been proposed for friction compensation [2]–[19]. Most of them are based on a friction model, for example on the simple Coulomb model [2]–[10], or on the more sophisticated LuGre model [11]–[13]. Such models approximate the behavior of the friction force with varying accuracy and complexity. Generally, the model complexity grows when models get more representative, requiring more extensive parameter estimation. To avoid the complicated estimation problem associated with these parameters, much research has been done on compensation methods that rely on the relatively simple Coulomb friction model [2]–[6], [8]–[10], [20], [21]. In the approach of [2], an observer is used for the on-line identification of the Coulomb friction coefficient. Asymptotic stability of the scheme is proven for the case when the true friction behaves according to the assumed Coulomb model and the velocity is bounded away from zero. In [4] and [5], compensation methods have been proposed which relax the constraint on the velocity. In both papers, global asymptotic stability of the position, velocity and Coulomb friction parameter estimate is claimed. However, asymptotic convergence of this parameter estimate cannot be guaranteed for zero velocities, which means that tracking errors may persist for constant references. The difficulty of achieving convergence for zero velocity is a direct result of the friction model assumed, which is based on a signum function.

In the papers [2], [4], [5], the rationale behind the definition of the signum function and hence the behavior of the friction model is overlooked. For example, at zero velocity, the signum function equals zero while it is known that the break-away force has to be overcome before motion actually occurs. This definition also makes it impossible to prove globally asymptotic convergence of the friction parameter estimate. When the signum function equals zero, the convergence of the Coulomb friction parameter estimate cannot be guaranteed [6]. In [6], a more realistic definition of the signum function is presented: the signum function depends, besides the velocity, on the total control input and on the Coulomb friction parameter. It is, however, assumed that the actual value of the signum function is always exactly equal to its modeled value. Exact modeling is only possible if all the input variables (velocity, total control input and Coulomb friction parameter) are known. This again turns out to be an unrealistic assumption because the Coulomb friction coefficient is unknown.

In the methods discussed so far, the Coulomb friction parameter is assumed to be constant. However, in reality, the friction force is not constant and depends on other variables like the velocity of the moving body. In later works, methods have been proposed to meet these properties. [8] focused on applications in which the friction force is assumed to be periodic with respect to time. Later, situations have been considered in which the friction force is periodic with respect to position [9]. Recently, a compensation method has been proposed that allows the friction to be generally time-varying [10]. This method is in essence similar to the one

K.A.J. Verbert and R. Babuška are with the Delft Center for Systems and Control (DCSC), Delft University of Technology, Mekelweg 2, 2628 CD Delft, The Netherlands. Email: {k.a.j.verbert, r.babuska}@tudelft.nl

R. Tóth is with the Control Systems Group, Department of Electrical Engineering, Eindhoven University of Technology, P.O. Box 513, 5600 MB, Eindhoven, The Netherlands, email: R.Toth@tue.nl.

proposed in [22]. Also in these works, no attention is paid to the definition of the signum function and its consequences for the stability analysis.

In this paper, we propose an adaptive compensation method that requires no friction modeling. An attractive feature of such a model-free approach over extensive model-based methods, like the LuGre-model-based compensators, is the ease of its implementation on different systems. Approaches based on extensive friction models require that for each system, a time-consuming, identification-based modeling phase needs to be carried out, which requires considerable user expertise. Moreover, most mechanical systems suffer from position-dependent friction, which cannot be easily included in the available friction models. This newly proposed method, which is an improved form of the methods proposed in [8], [9] and [10], overcomes the limitations for zero-velocity tracking as outlined above. The main contribution lays in the introduction of a physically realistic form of the signum function and the analysis of the resulting closed-loop stability. More specifically, we:

1) propose a realistic and useful definition of the signum function;
2) prove asymptotic stability of the proposed adaptive scheme;
3) demonstrate the performance of the compensation scheme via simulations and real-world experiments.

The paper is organized as follows: In Section II, the principal idea of the compensator is introduced. In Section III, the closed-loop system behavior is analyzed and next, in Section IV, we present the stability analysis of the closed-loop system. Issues regarding the discrete-time implementation and properties of the overall approach are discussed in Section VI. To validate the performance of the compensator, simulations and experiments are performed, which are presented in Section VII. Finally, conclusions and perspectives of future work are given in Section VIII.

II. The adaptive friction compensator

Consider the following motion control problem:

$$m\ddot{x}(t) + b\dot{x}(t) = u_{\mathrm{c}}(t) - F_{\mathrm{f}}\big(\dot{x}(t), u_{\mathrm{c}}(t), k_{\mathrm{c}}(t)\big), \qquad (1)$$

with $\ddot{x}(t)$ the acceleration of a mass $m > 0$ in the horizontal direction, $b \geq 0$ the viscous friction coefficient, $u_{\mathrm{c}}(t)$ the control input, and $F_{\mathrm{f}}\big(\dot{x}(t), u_{\mathrm{c}}(t), k_{\mathrm{c}}(t)\big)$ the friction force, which is modeled as:

$$F_{\mathrm{f}}\big(\dot{x}(t), u_{\mathrm{c}}(t), k_{\mathrm{c}}(t)\big) = k_{\mathrm{c}}(t)\sigma_0\big(\dot{x}(t), u_{\mathrm{c}}(t), k_{\mathrm{c}}(t)\big), \qquad (2)$$

with $k_{\mathrm{c}}(t) \geq 0$ a time-varying friction parameter and σ_0 the signum function defined as [6]:

$$\sigma_0\big(\dot{x}(t), u_{\mathrm{c}}(t), k_{\mathrm{c}}(t)\big) = \begin{cases} 1 & \text{if } \dot{x}(t) > 0 \text{ or } \big(\dot{x}(t) = 0 \text{ and } u_{\mathrm{c}}(t) > k_{\mathrm{c}}(t)\big), \\ -1 & \text{if } \dot{x}(t) < 0 \text{ or } \big(\dot{x}(t) = 0 \text{ and } u_{\mathrm{c}}(t) < -k_{\mathrm{c}}(t)\big), \\ \frac{u_{\mathrm{c}}(t)}{k_{\mathrm{c}}(t)} & \text{if } \dot{x}(t) = 0 \text{ and } |u_{\mathrm{c}}(t)| \leq k_{\mathrm{c}}(t). \end{cases} \qquad (3)$$

Important properties of this friction model (2)-(3) are that it does not require detailed friction modeling, while it still includes a realistic representation of the friction at zero velocity. At zero velocity, the friction force opposes the driving forces. So, for $\dot{x}(t) = 0$ in (1), it must hold that $u_{\mathrm{c}}(t) - F_{\mathrm{f}}\big(\dot{x}(t), u_{\mathrm{c}}(t), k_{\mathrm{c}}(t)\big) = 0$ unless $|u_{\mathrm{c}}(t)| > k_{\mathrm{c}}(t)$, in which case motion is initiated. Furthermore, as $k_{\mathrm{c}}(t)$ is time-varying, this model can represent a large family of friction behaviors.

The control input $u_{\mathrm{c}}(t)$ is composed of two terms: a 'nominal' control action $u(t)$ and a friction compensation action $w(t)$:

$$u_{\mathrm{c}}(t) = u(t) + w(t). \qquad (4)$$

The nominal control input $u(t)$ is chosen as a PD control law extended with feedforward velocity and acceleration terms to achieve good tracking performance for different types of reference signals. This is a further generalization of the control laws used in [8]–[10], [22]:

$$u(t) = \underbrace{m\alpha\lambda}_{K_{\mathrm{p}}} e_{\mathrm{x}}(t) + \underbrace{\big((\alpha+\lambda)m - b\big)}_{K_{\mathrm{d}}} \dot{e}_{\mathrm{x}}(t) + b\dot{x}_{\mathrm{d}}(t) + m\ddot{x}_{\mathrm{d}}(t), \qquad (5)$$

where $\alpha, \lambda \in \mathbb{R}^+$ are the tuning parameters of the controller, namely $-\alpha$ and $-\lambda$ are the closed-loop poles in the nominal situation when the friction is absent or perfectly compensated. Note that to calculate K_{p} and K_{d}, the system parameters m and b must be known.

To cancel the effect of friction, $w(t)$ is defined as[1]:

$$w(t) = \hat{k}_{\mathrm{c}}(t)\sigma\big(\dot{x}(t), u_{\mathrm{c}}(t), \hat{k}_{\mathrm{c}}(t)\big), \qquad (6)$$

where $\hat{k}_{\mathrm{c}}(t) \geq 0$ is a model-free estimate of the friction parameter $k_{\mathrm{c}}(t)$ and the signum function $\sigma\big(\dot{x}(t), u_{\mathrm{c}}(t), \hat{k}_{\mathrm{c}}(t)\big)$ is defined as:

$$\sigma\big(\dot{x}(t), u_{\mathrm{c}}(t), \hat{k}_{\mathrm{c}}(t)\big) = \begin{cases} 1 & \text{if } \dot{x}(t) > 0 \text{ or } \big(\dot{x}(t) = 0 \text{ and } u_{\mathrm{c}}(t) > \hat{k}_{\mathrm{c}}(t)\big), \\ -1 & \text{if } \dot{x}(t) < 0 \text{ or } \big(\dot{x}(t) = 0 \text{ and } u_{\mathrm{c}}(t) < -\hat{k}_{\mathrm{c}}(t)\big), \\ 0 & \text{if } \dot{x}(t) = 0 \text{ and } |u_{\mathrm{c}}(t)| \leq \hat{k}_{\mathrm{c}}(t). \end{cases} \qquad (7)$$

The differences between $\sigma\big(\dot{x}(t), u_{\mathrm{c}}(t), \hat{k}_{\mathrm{c}}(t)\big)$ and $\sigma_0(\dot{x}(t), u_{\mathrm{c}}(t), k_{\mathrm{c}}(t))$ used in the friction model (2) are that $k_{\mathrm{c}}(t)$ is replaced by $\hat{k}_{\mathrm{c}}(t)$ and that for $\dot{x} = 0$ and $u_{\mathrm{c}}(t) \leq |\hat{k}_{\mathrm{c}}(t)|$, the value of the signum function σ is set to 0 instead of $\frac{u_{\mathrm{c}}(t)}{\hat{k}_{\mathrm{c}}(t)}$.

In contrast to the standard definition of the signum function used in other works [2]–[10], this definition ensures an adequate compensation action, even at zero velocity. The problem with the standard definition of the signum function is that it is zero for zero velocity, regardless of $u_{\mathrm{c}}(t)$ acting on the system. So, when the system comes to rest in an undesired position, the compensation action is zero by definition. When also the nominal controller is not able to initiate any motion, the system stays in this undesired position.

As the definition of the signum function given by (7) is not directly suited for practical purposes, we derive an equivalent definition that is practically useful. For the sake of brevity, in the sequel, we omit the arguments of the functions σ and σ_0

[1]Note that computing $w(t)$ according to (6) requires the knowledge of $u_{\mathrm{c}}(t)$, which is not available. However, we use $\sigma\big(\dot{x}(t), u_{\mathrm{c}}(t), \hat{k}_{\mathrm{c}}(t)\big)$ only for illustration purpose. Later, in this paper, an alternative, but equivalent definition of the signum function is derived that is useful for practical purposes.

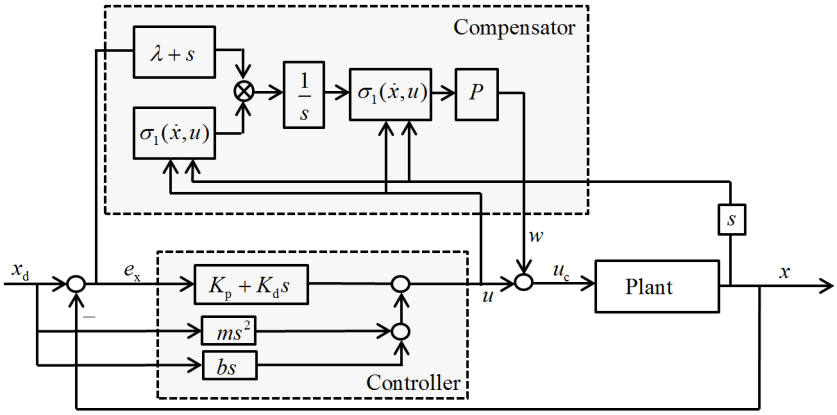

Fig. 1: The friction compensation scheme.

and we denote by $\sigma(t)$ and $\sigma_0(t)$ their time-varying nature where needed.

Because $w(t) = \hat{k}_c(t)$ if $\sigma(t) = 1$, see (6), it follows from (4), that $u_c(t) > \hat{k}_c(t)$ if and only if $u(t) > 0$. Similarly, for $\sigma(t) = -1$, $u_c(t) < -k_c(t)$ if and only if $u(t) < 0$. Finally, if $u_c(t) \leq |\hat{k}_c(t)|$, it follows that $u(t) = 0$. This last condition clarifies why one can set the value of the signum function σ to zero in this mode. When the system is at rest and the nominal controller commands a zero control action ($u(t) = 0$), no compensation is needed. Therefore, a realistic and useful definition of the signum function to be used in the compensator is:

$$\sigma_1\big(\dot{x}(t), u(t)\big) = \begin{cases} 1 & \text{if } \dot{x}(t) > 0 \text{ or } \big(\dot{x}(t) = 0 \text{ and } u(t) > 0\big), \\ -1 & \text{if } \dot{x}(t) < 0 \text{ or } \big(\dot{x}(t) = 0 \text{ and } u(t) < 0\big), \\ 0 & \text{if } \dot{x}(t) = 0 \text{ and } u(t) = 0. \end{cases} \tag{8}$$

Note that for the controller (4), σ_1 as defined in (8) is equivalent to σ as specified in (7). Now, the compensation action $w(t)$ can be rewritten as:

$$w(t) = \hat{k}_c(t)\sigma_1\big(\dot{x}(t), u(t)\big). \tag{9}$$

To determine $\hat{k}_c(t)$, the following update law [10] is used:

$$\dot{\hat{k}}_c(t) = P\sigma_1\big(\dot{x}(t), u(t)\big)[\dot{e}_x(t) + \lambda e_x(t)], \tag{10}$$

with $P, \lambda \in \mathbb{R}^+$ user-defined tuning parameters, with λ the same parameter as in the control law (5), and $e_x(t)$ the position error defined as:

$$e_x(t) = x_d(t) - x(t), \tag{11}$$

with $x_d(t)$ the desired position.

Combining (5) and (9), the total control input becomes:

$$u_c(t) = K_p e_x(t) + K_d \dot{e}_x(t) + b\dot{x}_d(t) + m\ddot{x}_d(t) + \hat{k}_c(t)\sigma_1\big(\dot{x}(t), u(t)\big). \tag{12}$$

The overall compensation scheme is shown in Figure 1.

III. Closed-loop system analysis

Applying the adaptive control law (12) to the plant (1) results in the following closed-loop dynamics:

$$\ddot{x}(t) = \frac{u_c(t) - k_c(t)\sigma_0\big(\dot{x}(t), u_c(t), k_c(t)\big) - b\dot{x}}{m}, \tag{13a}$$

$$\dot{\hat{k}}_c(t) = P\sigma_1\big(\dot{x}(t), u(t)\big)[\dot{e}_x(t) + \lambda e_x(t)], \tag{13b}$$

with $e_x(t)$, $u(t)$, and $u_c(t)$ as defined in (11), (5), (12). In the sequel, we assume that the system parameters m and b are known with a reasonable accuracy so that the nominal control law (5) can be designed.

Due to the signum functions σ_0 and σ_1, the closed-loop system is a hybrid system whose behavior can be described by several modes and transitions between these modes. Both the 'true' signum function σ_0 and the compensator signum function σ_1 can be in five different modes. These modes are given in Tables I and II, respectively.

TABLE I: Modes of $\sigma_0(\dot{x}(t), u_c(t), k_c(t))$.

Mode	$\dot{x}(t)$	$u_c(t)$	σ_0
M1	$(-\infty, 0)$	$\mathbb{R}$	-1
M2	0	$\big(-\infty, -k_c(t)\big)$	-1
M3	0	$[-k_c(t), k_c(t)]$	$[-1,\ 1]$
M4	0	$\big(k_c(t), \infty\big)$	1
M5	$(0, \infty)$	$\mathbb{R}$	1

TABLE II: Modes of $\sigma_1(\dot{x}(t), u(t))$.

Mode	$\dot{x}(t)$	$u(t)$	σ_1
M′1	$(-\infty, 0)$	$\mathbb{R}$	-1
M′2	0	$(-\infty, 0)$	-1
M′3	0	0	0
M′4	0	$(0, \infty)$	1
M′5	$(0, \infty)$	$\mathbb{R}$	1

The modes of σ_0 (abbreviated as M in the sequel) are interpreted as follows: M1 and M5 describe sliding motion for negative and positive velocities respectively, M3 is the stiction mode and M2 and M4 are break-away modes (transition between stiction and sliding). The modes of the two signum functions are not independent as only certain combinations are possible. For $\dot{x}(t) \neq 0$, both signum functions are in the same mode by definition. Furthermore, it is not possible that σ_1 is in M′3 (i.e. $\sigma_1 = 0$), while $\sigma_0 \neq 0$ (when $\dot{x}(t) = u(t) = \sigma_1 = 0$, then $u_c(t) = 0$ and from (3) it follows that $\sigma_0(t) = 0$). Finally, it is not possible that one of the signum functions is in Mode 2 and the other is in Mode 4 This leaves only 7 combinations in which the closed-loop system can be: the first 5 combinations are those in which the system and the compensator are in the same mode, and the last two are those in which the system, σ_0, is in M3 while the compensator, σ_1, is in M′2 or M′4.

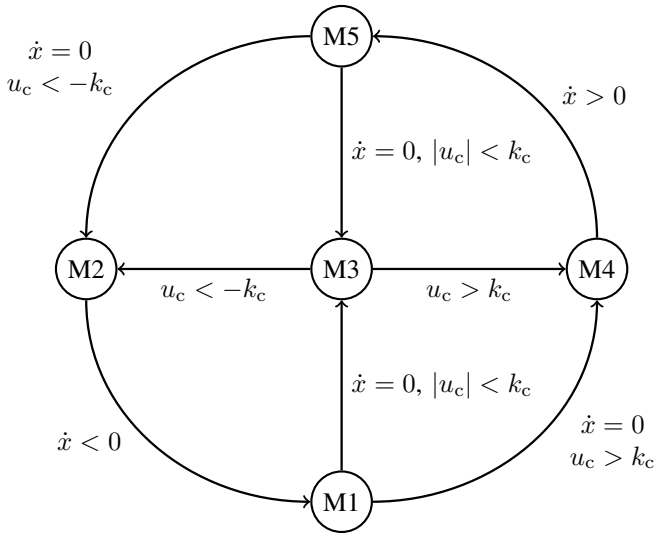

Fig. 2: Schematic overview of the different modes of $\sigma_0\big(\dot{x}(t), u_c(t), k_c(t)\big)$ and the possible transitions between these modes.

The system is also constrained in its switching possibilities. The signum functions cannot arbitrarily switch between their modes. For the compensator signum function σ_1, all transitions are possible except the direct transitions between M′1 and M′5 and between M′2 and M′4. The 'true' signum function σ_0 is more constrained in its transition possibilities. The possible transitions are illustrated in Figure 2.

The other transitions are physically impossible as will be explained next. First, it is shown that the 'true' signum function cannot stay in M2 or M4. These modes only serve to bring the system from M3 to M1 or M5. In addition, we show that the transitions M4 → M1 and M2 → M5 are excluded.

Lemma 1. *$\sigma_0\big(\dot{x}(t), u_c(t), k_c(t)\big)$ cannot stay in* M2 *or* M4 *and neither can switch from* M4 *to* M1 *and from* M2 *to* M5*.*

Proof. To remain in M2 or M4, both $\dot{x}(t)$ and $\ddot{x}(t)$ have to be equal to zero. This however conflicts with the conditions to be in M2 or M4. For example, to be in M4, it must hold that $u_c(t) > k_c(t)$. This results in:

$$m\ddot{x}(t) + b\dot{x}(t) = u_c(t) - \underbrace{F_f\big(\dot{x}(t), u_c(t), k_c(t)\big)}_{k_c(t)} > 0. \quad (14)$$

From (14) we can conclude that the system cannot stay in M4 and also cannot move to M1. Analogously, it can be proven that the system cannot stay in M2 and that the transition M2 → M5 is excluded. □

From this result, it can also be concluded that the transitions M4 → M3 and M2 → M3 cannot be executed because they require zero acceleration in modes M2 and M4, which is shown to be impossible. It also directly follows that the transitions M1 → M2 and M5 → M4 are not possible because they require either a zero acceleration in M2 and M4 or the execution of the transition M4 → M1 or M2 → M5.

Finally, transitions M3 → M5 and M3 → M1 are also not possible as shown by the following lemma.

Lemma 2. *$\sigma_0\big(\dot{x}(t), u_c(t), k_c(t)\big)$ cannot directly switch from* M3 *to* M5 *and from* M3 *to* M1*.*

Proof. To leave M3, the acceleration has to become unequal to zero. However, in M3, $\ddot{x}(t) = 0$, because in this mode $\ddot{x}(t)$ is constrained to be:

$$m\ddot{x}(t) = u_c(t) - \underbrace{k_c(t)\sigma_0\big(\dot{x}(t), u_c(t), k_c(t)\big)}_{u_c(t)} = 0. \quad (15)$$

Therefore, the transition M3 → M1 is only possible via M2, and the transition M3 → M5 is only possible via M4. □

IV. Stability analysis

In this section, stability of the adaptive compensation scheme is discussed. This analysis shows that the adaptive compensator will asymptotically cancel the effect of the friction force without destabilizing the nominal control loop. The technicalities of the proof require detailed insight into the following two situations:

Situation 1: Signum functions in the same mode When the plant and the compensator are in the same mode, it holds that $\sigma_1(t) = \sigma_0(t)$ (see Section III). The closed-loop system equations (13) simplify to:

$$\ddot{x}(t) = \frac{\hat{k}_c(t) - k_c(t)}{m}\sigma_1(t) + \alpha\lambda e_x(t) + (\alpha + \lambda)\dot{e}_x(t) + \ddot{x}_d(t), \quad (16a)$$

$$\dot{\hat{k}}_c(t) = P\sigma_1(t)\big(\dot{e}_x(t) + \lambda e_x(t)\big). \quad (16b)$$

The error dynamics become:

$$\begin{bmatrix} \dot{e}_x(t) \\ \ddot{e}_x(t) \\ \dot{e}_a(t) \end{bmatrix} = A(t)\begin{bmatrix} e_x(t) \\ \dot{e}_x(t) \\ e_a(t) \end{bmatrix} + \begin{bmatrix} 0 \\ 0 \\ 1 \end{bmatrix}\dot{k}_c(t), \quad (17)$$

with

$$A(t) = \begin{bmatrix} 0 & 1 & 0 \\ -\alpha\lambda & -(\lambda+\alpha) & \frac{\sigma_1(t)}{m} \\ -P\lambda\sigma_1(t) & -P\sigma_1(t) & 0 \end{bmatrix},$$

and $e_a(t)$ defined as $k_c(t) - \hat{k}_c(t)$.

Situation 2: Signum functions in different modes In this situation, the compensator and the plant are in different modes. The following combinations are possible (see Section III):

$$\text{System in M3, compensator in M}'2 \quad (18a)$$

$$\text{System in M3, compensator in M}'4. \quad (18b)$$

In this situation, the following equations hold:

$$\dot{x}(t) = 0, \quad (19a)$$

$$\sigma_1(t) = \begin{cases} -1 & \text{for combination (18a),} \\ 1 & \text{for combination (18b),} \end{cases} \quad (19b)$$

$$\sigma_0(t) = \frac{u_c(t)}{k_c(t)}. \quad (19c)$$

The closed-loop system equations simplify to:

$$\ddot{x}(t) = 0, \quad (20a)$$

$$\dot{\hat{k}}_c(t) = P\sigma_1(t)\big(\dot{e}_x(t) + \lambda e_x(t)\big). \quad (20b)$$

The error dynamics become:

$$\begin{bmatrix} \dot{e}_x(t) \\ \ddot{e}_x(t) \\ \dot{e}_a(t) \end{bmatrix} = A(t)\begin{bmatrix} e_x(t) \\ \dot{e}_x(t) \\ e_a(t) \end{bmatrix} + \begin{bmatrix} 0 & 0 \\ 1 & 0 \\ 0 & 1 \end{bmatrix}\begin{bmatrix} \ddot{x}_d(t) \\ \dot{k}_c(t) \end{bmatrix}, \quad (21)$$

with

$$A(t) = \begin{bmatrix} 0 & 1 & 0 \\ 0 & 0 & 0 \\ -P\lambda\sigma_1(t) & -P\sigma_1(t) & 0 \end{bmatrix}.$$

To stay in these mode combinations, the following conditions must be satisfied:

$$u(t) \begin{cases} < 0 & \text{for combination (18a),} \\ > 0 & \text{for combination (18b),} \end{cases} \tag{22a}$$

$$e_{\mathrm{a}}(t) > 0. \tag{22b}$$

This last condition results from (3) and (7). If $\hat{k}_{\mathrm{c}}(t) > k_{\mathrm{c}}(t)$, it is not possible that the system is in M3 while the compensator is not.

From the above analysis, it can be concluded that the non-linear closed-loop system (13) is equivalent to the following piece-wise affine (PWA) system:

$$\begin{bmatrix} \dot{e}_{\mathrm{x}}(t) \\ \ddot{e}_{\mathrm{x}}(t) \\ \dot{e}_{\mathrm{a}}(t) \end{bmatrix} = A_i \begin{bmatrix} e_{\mathrm{x}}(t) \\ \dot{e}_{\mathrm{x}}(t) \\ e_{\mathrm{a}}(t) \end{bmatrix} + B_i \begin{bmatrix} \ddot{x}_{\mathrm{d}}(t) \\ \dot{k}_{\mathrm{c}}(t) \end{bmatrix}, \tag{23}$$

with i the modes as defined in Table II and:

$$A_1 = \begin{bmatrix} 0 & 1 & 0 \\ -\alpha\lambda & -(\lambda+\alpha) & -\frac{1}{m} \\ P\lambda & P & 0 \end{bmatrix}, \quad B_1 = \begin{bmatrix} 0 & 0 \\ 0 & 0 \\ 0 & 1 \end{bmatrix},$$

$$A_2 = \begin{bmatrix} 0 & 1 & 0 \\ 0 & 0 & 0 \\ P\lambda & P & 0 \end{bmatrix}, \quad B_2 = \begin{bmatrix} 0 & 0 \\ 1 & 0 \\ 0 & 1 \end{bmatrix},$$

$$A_3 = \begin{bmatrix} 0 & 1 & 0 \\ -\alpha\lambda & -(\lambda+\alpha) & 0 \\ 0 & 0 & 0 \end{bmatrix}, \quad B_3 = B_1,$$

$$A_4 = \begin{bmatrix} 0 & 1 & 0 \\ 0 & 0 & 0 \\ -P\lambda & -P & 0 \end{bmatrix}, \quad B_4 = B_2,$$

$$A_5 = \begin{bmatrix} 0 & 1 & 0 \\ -\alpha\lambda & -(\lambda+\alpha) & \frac{1}{m} \\ -P\lambda & -P & 0 \end{bmatrix}, \quad B_5 = B_1.$$

Because the error dynamics of the closed-loop system (13) can be written as a linear hybrid system (23), we can use linear stability theory to proof stability of the closed-loop system. To prove bounded-input-bounded-output stability of the linear system (23), it is sufficient to prove that the equilibrium point $\mathbf{x}_0 = [\,0\ 0\ 0\,]^\top$ of:

$$\begin{bmatrix} \dot{e}_{\mathrm{x}}(t) \\ \ddot{e}_{\mathrm{x}}(t) \\ \dot{e}_{\mathrm{a}}(t) \end{bmatrix} = A_i \begin{bmatrix} e_{\mathrm{x}}(t) \\ \dot{e}_{\mathrm{x}}(t) \\ e_{\mathrm{a}}(t) \end{bmatrix}. \tag{24}$$

is globally uniformly stable [23]–[25]: So, to prove stability, we are allowed to assume that $\ddot{x}_{\mathrm{d}}(t) = \dot{k}_{\mathrm{c}}(t) = 0$, as in other cases linearity of error system implies boundedness.

Theorem 1 (Closed-loop stability)**.** *The equilibrium $\boldsymbol{x}_0 = [\,0\ 0\ 0\,]^\top$ of system* (24) *is globally uniformly Lyapunov stable and locally uniformly asymptotically stable.*

Proof. Consider the following Lyapunov function:

$$V\big(\mathbf{x}(t)\big) = \mathbf{x}(t)^\top \underbrace{\begin{bmatrix} \frac{1}{2}(\lambda^2+2\alpha\lambda) & \frac{1}{2}\lambda & 0 \\ \frac{1}{2}\lambda & \frac{1}{2} & 0 \\ 0 & 0 & \frac{1}{2Pm} \end{bmatrix}}_{M} \mathbf{x}(t), \tag{25}$$

with $\mathbf{x}(t) = [\ e_{\mathrm{x}}(t) \quad \dot{e}_{\mathrm{x}}(t) \quad e_{\mathrm{a}}(t)\ ]^\top$. This Lyapunov function $V(\mathbf{x}(t))$ is positive definite and descredent w.r.t. $\mathbf{x}_0$, which can be proven as follows: $V(\mathbf{x}(t))$ is positive definite if M is positive definite. This is the case if all eigenvalues of M are strictly positive. The eigenvalues of M are:

$$\begin{bmatrix} \psi_1 \\ \psi_2 \\ \psi_3 \end{bmatrix} = \begin{bmatrix} \frac{1}{2Pm} \\ \frac{(\lambda^2+2\alpha\lambda+1)+\sqrt{(\lambda^2+2\alpha\lambda-1)^2+4\lambda^2}}{4} \\ \frac{(\lambda^2+2\alpha\lambda+1)-\sqrt{(\lambda^2+2\alpha\lambda-1)^2+4\lambda^2}}{4} \end{bmatrix}. \tag{26}$$

It is obvious that the first two eigenvalues are strictly positive. The third eigenvalue is positive if:

$$(\lambda^2+2\alpha\lambda+1) - \sqrt{(\lambda^2+2\alpha\lambda-1)^2+4\lambda^2} > 0,$$
$$4(\lambda^2+2\alpha\lambda) > 4\lambda^2. \tag{27}$$

Because $2\alpha\lambda > 0$, this inequality always holds. Furthermore, $V(\mathbf{x}(t))$ is trivially continuous in the neighborhood of $\mathbf{x}_0$ and the descredent property is satisfied by $V(\mathbf{x}(t))$ being quadratic with bounded M. As $V(\mathbf{x}(t))$ is positive definite, descredent and continuous at the origin, according to Lyapunov's direct method, asymptotic stability holds if $\dot{V}(\mathbf{x}(t))$, defined as:

$$\dot{V}\big(\mathbf{x}(t)\big) = (\lambda^2+2\alpha\lambda)e_{\mathrm{x}}(t)\dot{e}_{\mathrm{x}}(t) +$$
$$\lambda e_{\mathrm{x}}(t)\ddot{e}_{\mathrm{x}}(t) + \lambda\dot{e}_{\mathrm{x}}^2(t) + \dot{e}_{\mathrm{x}}(t)\ddot{e}_{\mathrm{x}}(t) + \frac{1}{Pm}e_{\mathrm{a}}(t)\dot{e}_{\mathrm{a}}(t), \tag{28}$$

is negative along all state trajectories. However, as proven in [26], this requirement is conservative and not satisfied for all stable systems. In [26] it is shown that for asymptotic stability, it is sufficient to prove that the time-averaged Lyapunov function derivatives are negative along all state trajectories. According to this result, asymptotic stability of $\mathbf{x}_0 = [\,0\ 0\ 0\,]^\top$ of (24) is proven by showing that:

1) For $\sigma_1(t) = \sigma_0(t)$ (situation 1), $V(\mathbf{x}(t))$ is non-increasing and $\mathbf{x}(t)$ converges to the equilibrium $\mathbf{x}_e = [\,0\ 0\ e\,]^\top$ with:
$$e = \begin{cases} e_{\mathrm{a}}(0) & \text{if } e_{\mathrm{x}}(0) = \dot{e}_{\mathrm{x}}(0) = \dot{x}_{\mathrm{d}}(t) = 0, \\ 0 & \text{otherwise.} \end{cases}$$
2) When $\sigma_1(t_2) = \sigma_0(t_2)$ and $\mathrm{sgn}(e_{\mathrm{x}}(t_2)) \neq -\mathrm{sgn}(\dot{e}_{\mathrm{x}}(t_2))$, then $\sigma_1(t) = \sigma_0(t)\ \forall t \geq t_2$.
3) When $\sigma_1(t_1) \neq \sigma_0(t_1)$ and/or $\mathrm{sgn}(e_{\mathrm{x}}(t_1)) = -\mathrm{sgn}(\dot{e}_{\mathrm{x}}(t_1))$, then $\exists t_s \in (0,\infty)$ for which holds that $\sigma_1(t_s) = \sigma_0(t_s)$, $\mathrm{sgn}(t_s) \neq -\mathrm{sgn}(t_s)$, and that $V(\mathbf{x}(t_s)) < aV(\mathbf{x}(t_1))$ with $a < \infty$.

So, we show that at the beginning of the experiment $V(\mathbf{x}(t))$ may increase, but this possible increase is bounded and lasts only for a finite amount of time. From $t = t_s$, $V(\mathbf{x}(t))$ monotonically converges to zero. According to the result of [26], this means that there exists time instants $t_d \geq t_s \geq 0$, for which holds that:

$$\frac{1}{t_d - t_0}\int_{t_0}^{t_d} \dot{V}\big(\mathbf{x}(s)\big)ds \leq 0. \tag{29}$$

Because for $t > t_s$, it holds that $\dot{V}(t) \leq 0$, for t_d appropriately chosen, this inequality is also satisfied for all other intervals of length $\Delta = t_d - t_0$, i.e.:

$$\frac{1}{\Delta}\int_{t}^{t+\Delta} \dot{V}\big(\mathbf{x}(s)\big)ds \leq 0, \ \ \forall t \geq t_0, \tag{30}$$

i.e., the time-averaged Lyapunov function derivative is negative (semi)definite.

The correctness of the three above mentioned criteria is proven as follows:

1) Rewrite $\dot{V}(\mathbf{x}(t))$ as:
$$\dot{V}\big(\mathbf{x}(t)\big) = \big(\lambda e_{\mathrm{x}}(t) + \dot{e}_{\mathrm{x}}(t)\big)\big(\lambda \dot{e}_{\mathrm{x}}(t) + \ddot{e}_{\mathrm{x}}(t)\big) + \frac{1}{Pm} e_{\mathrm{a}}(t)\dot{e}_{\mathrm{a}}(t) + 2\alpha\lambda e_{\mathrm{x}}(t)\dot{e}_{\mathrm{x}}(t). \quad (31)$$
For the ease of notation, define $S(t) = \lambda e_{\mathrm{x}}(t) + \dot{e}_{\mathrm{x}}(t)$. By using (17), it can be shown that:
$$\dot{S}(t) = \frac{\sigma_1(t)}{m} e_{\mathrm{a}}(t) - \alpha S(t). \quad (32)$$
Then, $\dot{V}(\mathbf{x}(t))$ can be rewritten as:
$$\dot{V}\big(\mathbf{x}(t)\big) = S(t)\Big(\frac{\sigma_1(t)}{m} e_{\mathrm{a}}(t) - \alpha S(t)\Big) + \frac{1}{Pm} e_{\mathrm{a}}(t)\dot{e}_{\mathrm{a}}(t) + 2\alpha\lambda e_{\mathrm{x}}(t)\dot{e}_{\mathrm{x}}(t). \quad (33)$$
Using relation (16b), the term $\frac{1}{Pm} e_{\mathrm{a}}(t)\dot{e}_{\mathrm{a}}(t)$ can be written as $-S(t)\frac{\sigma_1(t)}{m} e_{\mathrm{a}}(t)$, resulting in:
$$\dot{V}\big(\mathbf{x}(t)\big) = -\alpha S^2(t) + 2\alpha\lambda e_{\mathrm{x}}(t)\dot{e}_{\mathrm{x}}(t)\,. \quad (34)$$
Now, we can prove that $\dot{V}(\mathbf{x}(t)) \leq 0$ by writing:
$$\begin{aligned}\dot{V}\big(\mathbf{x}(t)\big) &= -\alpha S^2(t) + 2\alpha\lambda e_{\mathrm{x}}(t)\dot{e}_{\mathrm{x}}(t), \\ &= -\alpha\big(\lambda^2 {e_{\mathrm{x}}}^2(t) + \dot{e}_{\mathrm{x}}^2(t)\big) \leq 0. \end{aligned} \quad (35)$$
As $\alpha, \lambda > 0$, based on (35), we can conclude global stability. To proof convergence, we use Lasalle's invariant set theorem: Because $\alpha > 0$ and $\lambda > 0$, $\dot{V}(\mathbf{x}(t))$ can only be equal to zero if $e_{\mathrm{x}}(t) = 0$ and $\dot{e}_{\mathrm{x}}(t) = 0$, which means that $e_{\mathrm{x}}(t)$, $\dot{e}_{\mathrm{x}}(t) \to 0$ as $t \to \infty$. To prove convergence of $e_{\mathrm{a}}(t)$, consider relation (32). Because $e_{\mathrm{x}}(t)$, $\dot{e}_{\mathrm{x}}(t) \to 0$ as $t \to \infty$, this relation can be written as:
$$\lim_{t\to\infty} \ddot{e}_{\mathrm{x}}(t) = \frac{\sigma_1(t)}{m} e_{\mathrm{a}}(t). \quad (36)$$
If $\ddot{e}_{\mathrm{x}}(t) \to 0$ as $t \to \infty$, then $\sigma_1(t) \neq 0$ implies that $e_{\mathrm{a}}(t) \to 0$ as $t \to \infty$. To prove that $\ddot{e}_{\mathrm{x}}(t) \to 0$ as $t \to \infty$, consider the following equality:
$$\dot{e}_{\mathrm{x}}(t) = \int_0^t \ddot{e}_{\mathrm{x}}(\tau)d\tau + \dot{e}_{\mathrm{x}}(0). \quad (37)$$
Because $\dot{e}_{\mathrm{x}}(t) \to 0$ as $t \to \infty$, we get:
$$\lim_{t\to\infty} \dot{e}_{\mathrm{x}}(t) = \lim_{t\to\infty} \int_0^t \ddot{e}_{\mathrm{x}}(\tau)d\tau + \dot{e}_{\mathrm{x}}(0) = 0. \quad (38)$$
If $\dot{e}_{\mathrm{x}}(0)$ is bounded, and given the fact that the closed-loop eigenvalues are real (i.e. $e_x(t)$ converges in a non-oscillating way), the above equation can only be true if $\lim_{t\to\infty} \ddot{e}_{\mathrm{x}}(t) = 0$. Therefore, it can be concluded that $\ddot{e}_{\mathrm{x}}(t) \to 0$ as $t \to \infty$ and that $e_{\mathrm{a}}(t) \to 0$ as $t \to \infty$ and $\sigma_1(t) \neq 0$. So, based on Lasalle's set theory, it can be concluded that $e_{\mathrm{x}}(t)$, $\dot{e}_{\mathrm{x}}(t)$ and $e_{\mathrm{a}}(t) \to 0$ as $t \to \infty$ except if $\sigma_1(t) = 0$. In the latter case, only convergence of $e_{\mathrm{x}}(t)$ and $\dot{e}_{\mathrm{x}}(t)$ can be proven, nothing can be said about $e_{\mathrm{a}}(t)$. However, this is not a disadvantage of the compensator, but a physical necessity we have implicitly taken into our formulation of the compensation law. We decided to take no action when there is no tracking error and the system is standstill, i.e., $\dot{x} = 0$. Remember the definition of $\sigma_1(t)$ given by (8). Hence, there is no need and possibility to adapt $\hat{k}_{\mathrm{c}}(t)$.

Each equilibrium $\mathbf{x}_e = [0\ 0\ e]^\top$ for which $e \neq 0$ is however unstable, i.e., its region of attraction is constrained to the equilibrium point itself and all state trajectories that start outside an unstable equilibrium converge to $\mathbf{x}_0 = [\,0\ 0\ 0\,]^\top$. So if $e_{\mathrm{x}}(0) \neq 0 \vee \dot{e}_{\mathrm{x}}(0) \neq 0$ the desired equilibrium $\mathbf{x}_0$ is reached. This can be verified as follows: $\sigma_1(t) = 0$ can only be true if both $\sigma_1(t)$ and $\sigma_0(t)$ are in mode 3. $M3$ can only be entered via $M1$ or $M5$ (see Section III), which implies that $|\sigma_1(t)| = 1$ just before entering $M3$. As $x(t)$ and $\dot{x}(t)$ can only change continuously, just before the final transition to M3, $e_{\mathrm{x}}(t)$ and $\dot{e}_{\mathrm{x}}(t)$ need to come infinitely close to zero. If $e_{\mathrm{x}}(t)$ and $\dot{e}_{\mathrm{x}}(t)$ converge to zero, also $\ddot{e}_{\mathrm{x}}(t)$ must converge to zero, see (38). Using (17), it then can be concluded that also $e_{\mathrm{a}}(t)$ must be infinitely close to zero, i.e. the system converges to the equilibrium x_0.

2) To stay in $M'2$ or $M'4$, it must hold that $\dot{x}(t) = \ddot{x}(t) = 0$, i.e., the force equilibrium $u(t) + w(t) = k_{\mathrm{c}}(t)\sigma_0(t)$ must be satisfied. If $\dot{k}_{\mathrm{c}}(t) = 0$, i.e., $k_{\mathrm{c}}(t) = c_1$ with c_1 a constant, then:
$$\max |k_{\mathrm{c}}(t)\sigma_0(t)| = c_1,$$
which is reached for $|\sigma_0(t)| = 1$, i.e., when $\dot{x}(t) \neq 0$. Consider the situation:
$$\begin{aligned} \dot{x}(t) &\neq 0 \quad \text{for } t \in (t_2 - a, t_2] \\ \dot{x}(t) &= 0 \quad \text{for } t \in (t_2, t_2 + b) \end{aligned} \quad (39)$$
with $a, b > 0$. Then, at $t = t_2$, it must hold that:
$$\begin{aligned} |u(t_2) + w(t_2)| &= |k_{\mathrm{c}}(t_2)\sigma_0(t_2)|, \\ |u(t_2) + w(t_2)| &= c_1, \end{aligned} \quad (40)$$
and at $t = t_2 + \epsilon_1$, with ϵ_1 infinitely small, it must hold that:
$$\begin{aligned} |u(t_2 + \epsilon_1) + w(t_2 + \epsilon_1)| &= |k_{\mathrm{c}}(t_2 + \epsilon_1)\sigma_0(t_2 + \epsilon_1)| \\ &\leq c_1 \end{aligned} \quad (41)$$
From (40) and (41), it follows that for the supposed situation, i.e., (39) equilibrium in the modes $M'2$ and $M'4$ would only be possible if $|u(t_2 + \epsilon_1) + w(t_2 + \epsilon_1)| \leq |u(t_2) + w(t_2)|$, i.e., if $\frac{d}{dt}|u(t) + w(t)| \leq 0$ in these modes. However, $\frac{d}{dt}|u(t) + w(t)|$ is guaranteed to be positive in modes $M'2$ and $M'4$ for either $x_d(t) = 0$ or for $x_d(t) \neq 0$ if $\mathrm{sgn}(e_{\mathrm{x}}(t)) \neq -\mathrm{sgn}(\dot{e}_{\mathrm{x}}(t))$, meaning that under the condition $\mathrm{sgn}(e_{\mathrm{x}}(t)) \neq -\mathrm{sgn}(\dot{e}_{\mathrm{x}}(t))$, the force equilibrium $u(t) + w(t) = k_{\mathrm{c}}(t)\sigma_0(t)$ cannot be satisfied in $M'2$ and $M'4$ when there exists $t_2 < t$ for which holds $\dot{x}(t_2) \neq 0$. This can be proven as follows:

$x_{\mathrm{d}}(t) = 0$:
Under this condition, when the compensator is in $M'2$ or $M'4$, it holds that $e_{\mathrm{x}}(t) \neq 0$ and $\dot{e}_{\mathrm{x}}(t) = 0$. Without loss of generality assume that $e_x(t) > 0$. In this case, $u(t) = m\alpha\lambda e_{\mathrm{x}}(t) > 0$. As $e_x(t)$ must be positive and constant to stay in $M'4$, $u(t)$ must be constant and positive too. Then, from (6), (10), and the fact that $\sigma_1(t) = 1$ for $\dot{x}(t) = 0 \wedge u(t) > 0$, it follows that $\dot{w}(t) > 0$, meaning that $\frac{d}{dt}(u(t) + w(t)) > 0$. As $\frac{d}{dt}(k_{\mathrm{c}}(t)\sigma_0(t)) \leq 0$, the force equilibrium cannot be satisfied. From this result, it follows that if $x_{\mathrm{d}}(t) = 0$, then $\sigma_1(t_2) = \sigma_0(t_2)$ implies $\sigma_1(t) = \sigma_0(t) \forall\, t > t_2$.

$x_{\mathrm{d}}(t) \neq 0 \wedge \mathrm{sgn}(e_{\mathrm{x}}(t)) \neq -\mathrm{sgn}(\dot{e}_{\mathrm{x}}(t))$**:**
Under these conditions, when the compensator is in mode $M'2$ or $M'4$, it holds that $\dot{e}_{\mathrm{x}}(t) \neq 0$. Without loss of generality, we assume that $\dot{e}_{\mathrm{x}}(t) > 0$ (and $e_{\mathrm{x}}(t) \geq 0$). Then, from (5), it follows that $u(t) > 0$ and increasing. From (6), (10), and the fact that $\sigma_1 = 1$ for $\dot{x}(t) = 0 \wedge u(t) > 0$, it follows that $\dot{w}(t) > 0$, meaning that $\frac{d}{dt}(u(t)+w(t)) > 0$. As $\frac{d}{dt}(k_{\mathrm{c}}(t)\sigma_0(t)) \leq 0$, the force equilibrium cannot be satisfied. Because of the stability result for $\sigma_0(t) = \sigma_1(t)$, the system will not move to a position for which holds that $\mathrm{sgn}(e_{\mathrm{x}}(t)) = -\mathrm{sgn}(\dot{e}_{\mathrm{x}}(t))$. Therefore, we can conclude that $\sigma_1(t_2) = \sigma_0(t_2) \wedge \mathrm{sgn}(e_{\mathrm{x}}(t_2)) \neq -\mathrm{sgn}(\dot{e}_{\mathrm{x}}(t_2))$ implies $\sigma_1(t) = \sigma_0(t) \, \forall \, t > t_2$.

3) We have to show that:
   a) If $\sigma_1(t_1) \neq \sigma_0(t_1) \wedge \mathrm{sgn}(e_{\mathrm{x}}(t_1)) \neq -\mathrm{sgn}(\dot{e}_{\mathrm{x}}(t_1))$ then $\exists t_s$ with $t_1 < t_s < \infty$ for which $\sigma_1(t_s) = \sigma_0(t_s) \wedge \mathrm{sgn}(e_{\mathrm{x}}(t_s)) \neq -\mathrm{sgn}(\dot{e}_{\mathrm{x}}(t_s))$;
   b) If $\sigma_1(t_1) \neq \sigma_0(t_1) \wedge \mathrm{sgn}(e_{\mathrm{x}}(t_1)) = -\mathrm{sgn}(\dot{e}_{\mathrm{x}}(t_1))$, then $\exists t_v < \infty$ for which $\mathrm{sgn}(e_{\mathrm{x}}(t_v)) \neq -\mathrm{sgn}(\dot{e}_{\mathrm{x}}(t_v))$ and/or $\sigma_1(t_v) = \sigma_0(t_v)$;
   c) $V(x(t_s)) < aV(x(t_1))$, with $a < \infty$, i.e., $V(x(t))$ remains bounded;

   are true, which can be proven as follows:
   a) Under these conditions, $\frac{d}{dt}|u(t)| \geq 0$ and $\frac{d}{dt}|w(t)| > 0$. So, if $k_{\mathrm{c}}(t)$ is finite, there is exist a moment $t_s > t_1$ at which the force equilibrium can no longer be satisfied, i.e. the system starts moving meaning that $\sigma_1(t_s) = \sigma_0(t_s) \wedge \mathrm{sgn}(e_{\mathrm{x}}(t_1)) \neq -\mathrm{sgn}(\dot{e}_{\mathrm{x}}(t_1))$.
   b) If $\sigma_1(t_1) \neq \sigma_0(t_1) \wedge \mathrm{sgn}(e_{\mathrm{x}}(t_1)) = -\mathrm{sgn}(\dot{e}_{\mathrm{x}}(t_1))$, then convergence to the desired position is guaranteed by the linear growth of $x_{\mathrm{d}}(t)$[2]. So, there exist a finite moment t_v at which $\mathrm{sgn}(e_{\mathrm{x}}(t_v)) = -\mathrm{sgn}(\dot{e}_{\mathrm{x}}(t_v))$ and/or $\sigma_1(t_v) \neq \sigma_0(t_v)$ no longer hold; Or the system stays at rest and due to the linear growth of $x_{\mathrm{d}}(t)$, at $t = t_v$, it no longer holds that $\mathrm{sgn}(e_{\mathrm{x}}(t)) = -\mathrm{sgn}(\dot{e}_{\mathrm{x}}(t))$. Or the total control input $(u(t) + w(t))$ becomes sufficiently large that motion is initiated, i.e., $\sigma_1(t_v) \neq \sigma_0(t_v)$ is no longer satisfied.
   c) As the friction force is finite, both $e_{\mathrm{x}}(t), \dot{e}_{\mathrm{x}}(t)$, and $e_{\mathrm{a}}(t)$ must be bounded to be in $M'2$ or $M'4$. Therefore $V(x(t_s)) < \infty$, i.e., $\exists a$ for which $V(\mathbf{x}(t_s)) < aV(\mathbf{x}(t_1))$. □

V. Comparison

In this section, we demonstrate the advantages of the proposed compensation scheme compared to the schemes proposed in [10], [22]. We compare with these methods because they do not require extensive friction modeling, just like our method. Furthermore, they use a friction model of the same structure. The only difference compared to the proposed method is that they are based on the standard signum function $\mathrm{sgn}(\dot{x}(t))$:

$$\mathrm{sgn}(\dot{x}(t)) = \begin{cases} -1 & \text{if } \dot{x}(t) < 0, \\ 0 & \text{if } \dot{x}(t) = 0, \\ 1 & \text{if } \dot{x}(t) > 0. \end{cases} \tag{42}$$

The problem of using $\mathrm{sgn}(\dot{x}(t))$ instead of $\sigma_1(\dot{x}(t), u(t))$ in the compensator equations (6), (10) is that in this case the compensator is inactive when the system is in standstill, i.e., for $\dot{x}(t) = 0$, it holds that $w(t) = \dot{\hat{k}}_{\mathrm{c}}(t) = 0$. As a consequence, compensation schemes based on $\mathrm{sgn}(\dot{x}(t))$ are not able to compensate for static friction forces. When $\dot{x}(t) = 0$ and the nominal control action $u(t)$ cannot initiate motion ($|u(t)| < k_{\mathrm{c}}(t)$) the system stays at rest, even if it is in an undesired position. Contrary, the newly proposed signum function $\sigma_1(\dot{x}(t), u(t))$ is only equal to zero when both $\dot{x}(t) = 0$ and $u(t) = 0$. So, when $\dot{x}(t) = 0$ and $u(t) \neq 0$ (indicating that there is static friction), the friction compensator is active.

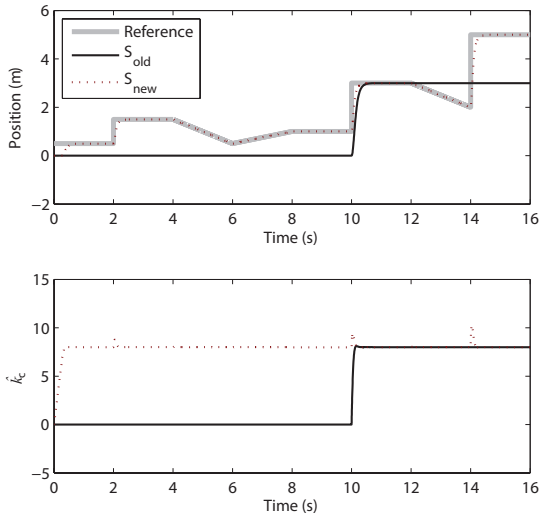

Fig. 3: Comparison of the newly proposed compensation scheme with a scheme based on the standard signum function.

To illustrate the differences mentioned, we simulate the system as defined by (12) and (13) (with $m = 0.007$, $b = 0.056$, $K_{\mathrm{p}} = 3.135$, $K_{\mathrm{d}} = 0.327$, $P = 5$, $\lambda = 10$, $\alpha = 45$) with $\sigma_1(\dot{x}(t), u(t))$ (hereafter referred to as $\mathrm{S_{new}}$) and with $\sigma_1(\dot{x}(t), u(t))$ replaced by $\mathrm{sgn}(\dot{x}(t))$ (hereafter referred to as $\mathrm{S_{old}}$). The results are given in Figure 3. Here, the friction is simulated according to (2) with $k_c(t) = 8$. At the start of the experiment, the errors $e_{\mathrm{x}}(t)$ and $\dot{e}_{\mathrm{x}}(t)$ are so small that the nominal controller does not initiate motion. As long as $|u(t)| < k_{\mathrm{c}}(t)$, $\mathrm{S_{old}}$ stays in its initial state. As $u(0) \neq 0$, $\hat{k}_{\mathrm{c}}(t)$ is directly updated in $\mathrm{S_{new}}$ and as soon as $e_{\mathrm{a}}(t)$ is sufficiently small (the exact convergence rate depends on the tuning of the parameters λ and P, see Section VII), the system starts moving towards the desired trajectory. At $t = 10$, the nominal control action $u(t)$ equals the static friction force and also $\mathrm{S_{old}}$ starts moving. As soon as $\dot{x}(t) \neq 0$, the friction compensator is activated and shortly after this moment the two systems behave identically. However, when the velocity becomes zero again, the same problem repeats, even though, at this moment, we have a perfect friction estimate, i.e. $e_{\mathrm{a}}(t) = 0$.

[2]Note that $\ddot{x}_d(t) \equiv 0 \implies \dot{x}_d(t) = c \in \mathbb{R}$ and if $\dot{x}_d(t) = 0$, then $\mathrm{sgn}(e_{\mathrm{x}}(t)) \neq -\mathrm{sgn}(\dot{e}_{\mathrm{x}}(t))$.

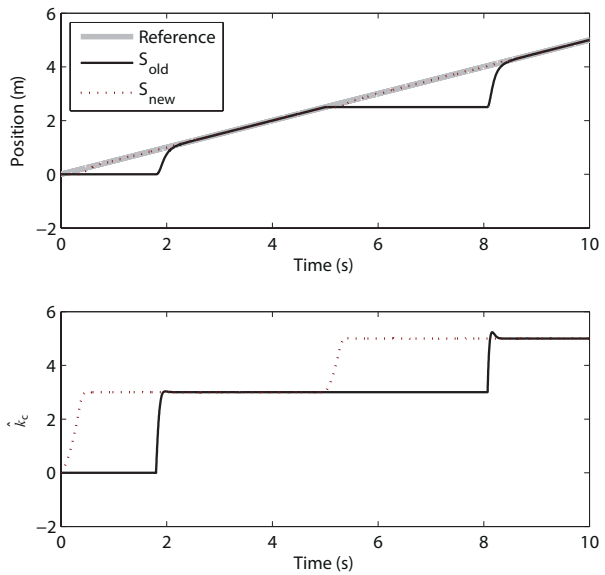

Fig. 4: Comparison of the two compensation schemes for time-varying friction behavior. At $t = 5$, the friction parameter $k_c(t)$ abruptly changes from 3 to 5.

This problem aggravates when the friction force is time-varying (as is illustrated in Figure 4 for tracking a ramp reference). As soon as the friction force suddenly increases, the velocity becomes zero. In this situation, $\mathrm{S_{new}}$ starts moving again as soon as $|w(t) + u(t)| > k_{\mathrm{c}}(t)$, whereas $\mathrm{S_{old}}$ starts moving when $|u(t)| > k_{\mathrm{c}}$.

From the above analysis, we conclude that the modified compensator performs significantly better, particularly for time-varying frictions forces and high-precision tasks.

VI. Practical implementation

The derivations so far have been provided in continuous-time. However, in simulations and real-world experiments, the system variables are only available at discrete time-instants. To make the adaptive compensation method suitable for numerical simulations and real-world implementation, the update law (10) has to be transformed to a difference equation. This can be done, for example, by using forward difference (Euler's method), backward difference, bilinear approximation (trapezoidal rule) or Runge Kutta approximation [27]. Here, we use the bilinear approximation because it is a relatively simple and accurate method which preserves the stability properties of the original differential equation. In this way, the friction parameter estimate $\hat{k}_{\mathrm{c}}(t)$ can be updated by:

$$\hat{k}_{\mathrm{c}}[k] = \hat{k}_{\mathrm{c}}[k-1] + \frac{T_{\mathrm{s}}}{2}\dot{\hat{k}}_{\mathrm{c}}[k] + \frac{T_{\mathrm{s}}}{2}\dot{\hat{k}}_{\mathrm{c}}[k-1], \qquad (43)$$

where $\dot{\hat{k}}_{\mathrm{c}}[k]$ is given by (10). The choice of the sampling rate $1/T_{\mathrm{s}}$ depends on the frequency content of the sampled signal, here $x(t)$. Generally, to obtain an accurate representation of $x(t)$, the sampling rate $1/T_{\mathrm{s}}$ should be 10-30 times higher than the highest frequency in $x(t)$.

As it is not a priori known what frequencies the adaptive compensator will invoke (e.g., stick-slip behavior can result in rapid changes in the velocity), it is best to chose T_{s} as small as possible. However, the minimal value of T_{s} is constrained by the computational time required by the control hardware.

Besides these discrete-time limitations, the following restrictions must be taken into account:

- The time delay between sensing the system output and applying the control input;
- Quantization errors;
- Errors due to unmodeled dynamics;
- Velocity estimation errors in the absence of a velocity sensor.

All of these limitations make the practical implementation less robust compared to the theoretical situation. However, most problems will not occur for a realistic practical setting and some problems can be avoided by making small adjustments to the scheme:

1) Introducing a dead-zone for the friction compensation action $w(t)$: In practice, $x(t)$ is never exactly equal to $x_{\mathrm{d}}(t)$. Due to this, the compensator remains active and $x(t)$ may start chattering around $x_{\mathrm{d}}(t)$. This can easily be solved by introducing a small error bound $|e_{\mathrm{x}}(t)| < \epsilon$ in which $w(t) = \dot{\hat{k}}_{\mathrm{c}}(t) = 0$.
2) As both the controller and the compensator are error-based, there is no clear separation between the control task and the compensator task when the reference $x_{\mathrm{d}}[k]$ is directly used in the compensator. In the case of sudden changes in the reference signal, the compensator not only reacts to errors due to friction, but also to errors due to the normal transient response of the system. To avoid this problem, the compensator can be fed by a reference signal $x_{\mathrm{d,f}}[k]$, obtained by filtering $x_{\mathrm{d}}[k]$ by the desired closed-loop dynamics.

The compensation algorithm, including these modifications, is given in Algorithm 1.

VII. Simulation and experimental results

In this section, the performance of the proposed adaptive friction compensation method is demonstrated via representative simulations and experimental studies. First, the compensation scheme is applied to a servo positioning system. Both simulation and real-world experimental results are given for this system. Next, experimental results are presented for the distal link of a 2-DOF robot manipulator.

A. Servo positioning system

To test the performance of the compensation method in a representative setting, a servo positioning system with an adjustable friction level is considered (see Figure 5). This system consists of a voltage-controlled DC motor which directly drives a plastic disc (CD-ROM). This system is designed to have a minimal level of friction, which is almost entirely of the viscous type, i.e., linearly proportional to the shaft angular velocity. A mechanical friction brake can be pressed against the back side of the CD-ROM, which introduces additional, manually adjustable, dry friction. Without this additional friction, the system dynamics are described by the following simplified linear model (neglecting the armature inductance):

$$\tau\ddot{q}(t) + \dot{q}(t) = k_{\mathrm{m}}u_{\mathrm{c}}(t), \qquad (44)$$

Algorithm 1 Adaptive friction compensation in discrete time

Input: Tuning parameters P and λ, sampling period T_s, filtered reference signal $x_{\mathrm{d,f}}$ and its derivative $\dot{x}_{\mathrm{d,f}}$, deadzone ϵ for the compensation action.

Initialize the state $[x[0]\ \dot{x}[0]]^\top$, the input $u[0]$ and the friction parameter estimate $\hat{k}_\mathrm{c}[0]$. Set $k = 1$.
repeat
  Measure system output $x[k]$.
  Measure $\dot{x}[k]$ or estimate it by using backward difference:

$$\dot{x}[k] \approx \frac{x[k] - x[k-1]}{T_\mathrm{s}}.$$

  Calculate the position error and its derivative:

$$e_\mathrm{x}[k] = x_{\mathrm{d,f}}[k] - x[k],$$
$$\dot{e}_\mathrm{x}[k] = \dot{x}_{\mathrm{d,f}}[k] - \dot{x}[k].$$

  Compute $\dot{\hat{k}}_\mathrm{c}[k]$:
  if $\dot{x}_\mathrm{d}[k] = 0$ and $|e_\mathrm{x}[k]| < \epsilon$ **then**

$$\dot{\hat{k}}_\mathrm{c}[k] = 0,$$

  else

$$\dot{\hat{k}}_\mathrm{c}[k] = P\sigma_1(\dot{x}[k], u[k])(\dot{e}_x[k] + \lambda e_x[k]).$$

  Update $\hat{k}_\mathrm{c}[k]$ using the trapezoidal rule:

$$\hat{k}_\mathrm{c}[k] = \hat{k}_\mathrm{c}[k-1] + \frac{T_\mathrm{s}}{2}\dot{\hat{k}}_\mathrm{c}[k-1] + \frac{T_\mathrm{s}}{2}\dot{\hat{k}}_\mathrm{c}[k].$$

  Compute the control input $u[k]$ (i.e., the control input without compensation).
  Compute the total control action $u_\mathrm{c}[k]$:
  if $\dot{x}_\mathrm{d}[k] = 0$ and $|e_\mathrm{x}[k]| < \epsilon$ **then**

$$u_\mathrm{c}[k] = u[k],$$

  else

$$u_\mathrm{c}[k] = u[k] + \hat{k}_\mathrm{c}[k]\sigma_1(\dot{x}[k], u[k]).$$

  Send the actual control input $u_\mathrm{c}[k]$ to the plant.
  $k \leftarrow k + 1$.
until end of experiment.

with $q(t)$ the angular position of the disc (fulfilling the same role as the position $x(t)$ previously), $u_\mathrm{c}(t)$ the input voltage and k_m and τ the characteristic motor parameters, lumping the influence of the torque constant, armature resistance, back-emf, viscous friction, and the moment of inertia. In state-space form, (44) can be given as:

$$\begin{bmatrix} \dot{q}(t) \\ \ddot{q}(t) \end{bmatrix} = \begin{bmatrix} 0 & 1 \\ 0 & -\frac{1}{\tau} \end{bmatrix} \begin{bmatrix} q(t) \\ \dot{q}(t) \end{bmatrix} + \begin{bmatrix} 0 \\ \frac{k_\mathrm{m}}{\tau} \end{bmatrix} u_\mathrm{c}(t). \quad (45)$$

Fig. 5: Servo positioning system with a manually adjustable level of friction (using the lever at the right side of the box).

With the armature inductance neglected, the friction torque can be directly related to voltage, so that the state-space model including friction becomes:

$$\begin{bmatrix} \dot{q}(t) \\ \ddot{q}(t) \end{bmatrix} = \begin{bmatrix} 0 & 1 \\ 0 & -\frac{1}{\tau} \end{bmatrix} \begin{bmatrix} q(t) \\ \dot{q}(t) \end{bmatrix} + \begin{bmatrix} 0 \\ \frac{k_\mathrm{m}}{\tau} \end{bmatrix} \big(u_\mathrm{c}(t) - V_\mathrm{f}(t)\big), \quad (46)$$

where $V_\mathrm{f}(t)$ is the voltage that generates a torque equal in magnitude to the friction torque. To control this system, the following PD-type control law is applied:

$$u_\mathrm{c}(t) = \underbrace{K_\mathrm{p}e_\mathrm{q}(t) + K_\mathrm{d}\dot{e}_\mathrm{q}(t) + \frac{1}{k_\mathrm{m}}\dot{q}_\mathrm{d}(t)}_{u(t)} + \underbrace{\hat{k}_\mathrm{c}(t)\sigma_1(\dot{q}(t), u(t))}_{w(t)}, \quad (47)$$

with:

$$K_\mathrm{p} = \frac{\tau}{k_\mathrm{m}}\alpha\lambda,$$
$$K_\mathrm{d} = \frac{\tau}{k_\mathrm{m}}(\alpha + \lambda) - \frac{1}{k_\mathrm{m}},$$

and $q_\mathrm{d}(t)$ the desired position, $\dot{q}_\mathrm{d}(t)$ the desired velocity and $e_\mathrm{q}(t) = q_\mathrm{d}(t) - q(t)$ the tracking error. The filtered position reference is obtained by filtering $q_\mathrm{d}(t)$ by the desired closed-loop dynamics:

$$Q_{\mathrm{d,f}}(s) = \frac{\lambda\alpha}{s^2 + (\lambda+\alpha)s + \lambda\alpha}Q_\mathrm{d}(s) + \frac{\lambda + \alpha}{s^2 + (\lambda+\alpha)s + \lambda\alpha}sQ_\mathrm{d}(s), \quad (48)$$

where $sQ_\mathrm{d}(s)$ is the desired velocity, which equals zero for step references.

We first run simulations in order to get insight into the behavior of the compensator and the effect of its tuning parameters. This knowledge is then used to tune the compensator for real-world experiments, which are reported next.

1) Simulations: In the simulations, the system model given in (46) is used with k_m and τ identified from data measured on the setup with low friction. The parameters are as follows: $k_\mathrm{m} = 17.8\,\mathrm{rad/s/V}$, $\tau = 0.124\,\mathrm{s}$, $\alpha\lambda = 450$, $\alpha + \lambda = 45$, and $\epsilon = 0.01\,\mathrm{rad}$. The sampling period is $T_\mathrm{s} = 0.0001\,\mathrm{s}$. Here, the parameters α and λ are tuned based on pole-placement ($-\alpha$ and $-\lambda$ are the desired closed-loop poles) while taking the restrictions on K_p and K_d, as given by (5), into account. The dead-zone parameter ϵ is tuned empirically and independently based on the desired accuracy in the light of the sensor resolution. For the simulations and the subsequent experiments, reference signals composed of step and ramp inputs, covering a wide range of velocities, including velocity reversals, are used (see Figures 6, 7, 8). In all simulations and experiments, the state is initialized as:

$$\begin{bmatrix} e_\mathrm{q}(0) & \dot{e}_\mathrm{q}(0) & \hat{k}_\mathrm{c}(0) \end{bmatrix}^\top = [\,0 \;\; 0 \;\; 0\,]^\top,$$

and in the simulations, a time-varying friction force is considered. The corresponding voltage is modeled as:

$$V_\mathrm{f}(t) = \begin{cases} 4\sigma_0\big(\dot{q}(t), u_\mathrm{c}(t), k_\mathrm{c}(t)\big) & \text{for } t < 10.5, \\ 6\sigma_0\big(\dot{q}(t), u_\mathrm{c}(t), k_\mathrm{c}(t)\big) & \text{for } t < 18, \\ 2\sigma_0\big(\dot{q}(t), u_\mathrm{c}(t), k_\mathrm{c}(t)\big) & \text{for } t \geq 18, \end{cases}$$

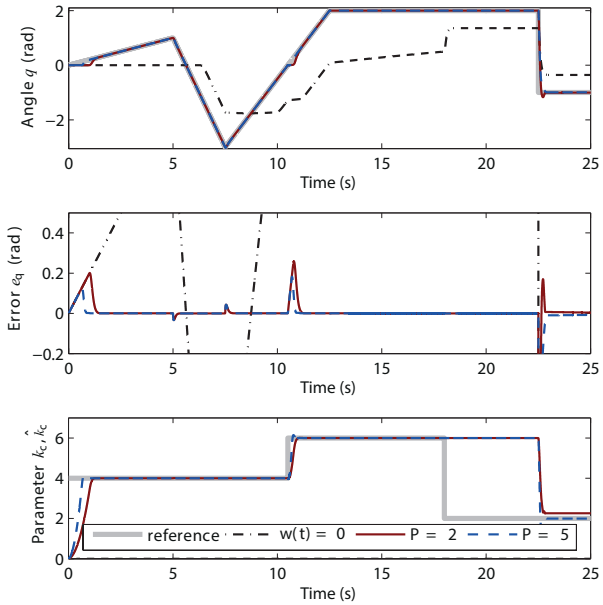

Fig. 6: Simulation results: effect of P on the compensation performance ($\lambda = 15$). In the bottom plot, "reference" refers to the true parameter k_c.

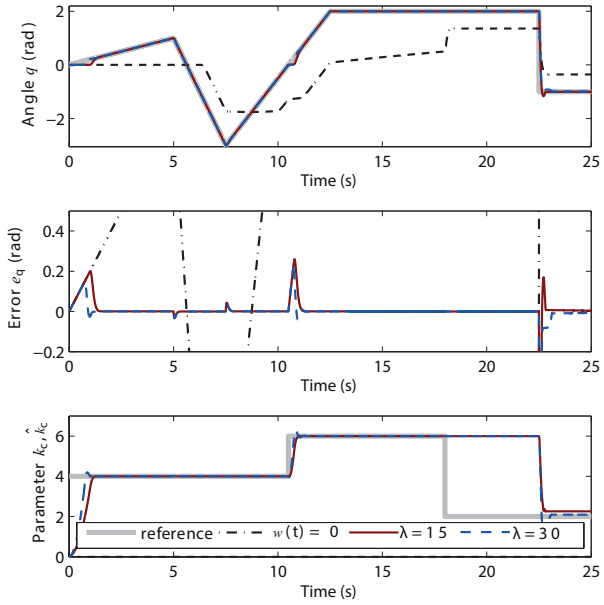

Fig. 7: Simulation results: effect of λ on the compensation performance ($P = 2$). In the bottom plot, "reference" refers to the true parameter k_c.

which corresponds to harsh step-changes of the friction. From the simulation results given in Figures 6 and 7, we can conclude that the compensator effectively eliminates the steady-state errors caused by friction. The value of the tuning parameter P influences the adaptation speed, i.e., the speed at which the compensator responds to tracking errors due to friction. This is illustrated in Figure 6: at the start of the experiment, the output corresponding to $P = 5$ converges faster to the reference signal than the output corresponding to $P = 2$. This difference is also visible at $t = 10.5$, where the magnitude of the friction torque changes. Finally, it can be concluded that the convergence properties of the friction parameter estimate $\hat{k}_c(t)$ are in agreement with the results of Section IV: $\hat{k}_c(t)$ converges to $k_c(t)$ unless $\dot{q}(t) = 0$ and $e_q(t) = 0$.

The tuning parameter λ determines the trade-off between position and velocity tracking. In Figure 7, we can see that larger λ results in faster convergence of the output to the desired position. When λ is chosen small, more weight is put on the minimization of the velocity error and therefore it takes more time to reach the desired position.

In summary, larger values of both tuning parameters make the compensator react faster to position and velocity errors. However, too large values will make the compensator sensitive to noise, possibly resulting in oscillations around the desired position. In real-life scenarios, the actual sensor noise levels will impose upper bounds on the feasible values of the tuning parameters P and λ.

2) Experiments: To test the performance in a real-world setting, experiments were conducted with the actual servo positioning system shown in Figure 5. The parameters used are: $\alpha = 30$, $T_s = 0.0025\,\mathrm{s}$ and $\epsilon = 0.01\,\mathrm{rad}$. From the results presented in Figure 8 we can conclude that the proposed scheme clearly outperforms a compensation-free control scheme. The large steady-state error, which occurs in

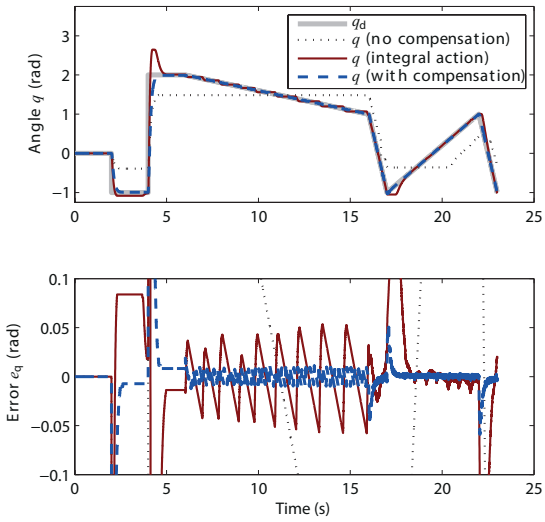

Fig. 8: Experimental results: servo positioning setup ($\lambda = 10$, $P = 50$).

the absence of a compensatory action, has almost completely disappeared. Furthermore, it can be seen that the proposed scheme outperforms integrator-based compensation both at velocity reversals and for low-velocity tracking, where integral control results in significant stick-slip behavior.

To illustrate the adaptability, an additional experiment is conducted in which the friction torque is changed manually at a number of time instants. This is done by changing the force (using the lever shown in Figure 5) by which the friction brake pushes against the disk. The results given in Figure 9 show that the adaptation is fast even under rapid and significant changes in the friction torque. The compensation action, plotted in the bottom panel of Figure 9, gives an indication of the friction variation. Note that a high value of P is required to track the rapidly varying friction torque.

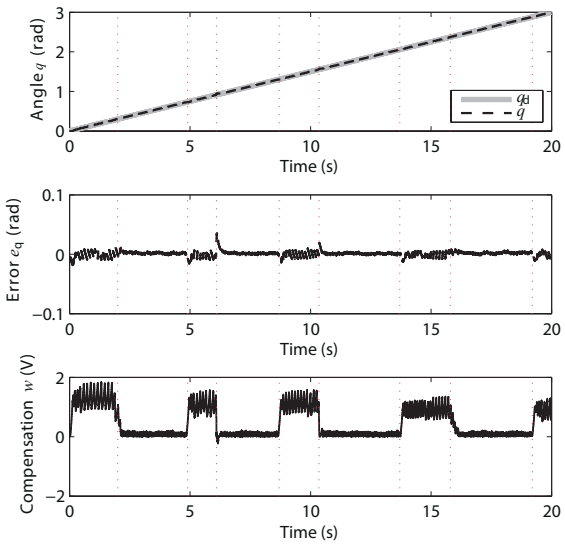

Fig. 9: Experimental results: servo positioning system. In this experiment, the friction torque is manually changed to test the compensator's performance when the friction torque is highly time-varying ($\lambda = 10$, $P = 50$). The dotted vertical lines indicate where the friction force is changed.

B. 2-DOF robot manipulator

In this section, we validate the compensation strategy on the distal link of a two degree of freedom robot arm (see Figure 10). We chose this system as it has a different type of actuators (Dynamixel RX-28 servomotors by Robotis) with different associated dynamics and friction characteristics. In contrast to the DC motor used in part A, the Dynamixel servomotors are equipped with gearboxes. The lengths of the links of this robot are $0.19\,\mathrm{m}$ (proximal link) and $0.06\,\mathrm{m}$ (distal link). The dynamics of the distal link can be well approximated by a linear model of the same form as the model used for the servo positioning system discussed in Section VII-A. The control and compensation scheme used is also identical to the one explained in Section VII-A. Here, the control gains K_p, K_d of the nominal controller (5) are designed by pole placement, where the design parameters are the desired natural frequency ω and the desired relative damping ζ. The following parameters are used: $k_\mathrm{m} = 7.87\,\mathrm{rad/s}^3$, $\tau = 0.011\,\mathrm{s}$, $\omega = 30\,\mathrm{rad/s}$, $\zeta = 0.9$ and $\epsilon = 0.02\,\mathrm{rad}$. The sampling period is $T_\mathrm{s} = 0.005\,\mathrm{s}$. In this case, the nominal control law is chosen as a PD controller, however, not exactly in the form of (5). More specifically, the closed-loop poles are complex and the friction compensator parameter λ is chosen independently of the nominal controller. Also in this case, the compensator performs well. Figure 11 shows the tracking results for the distal link. Again, the addition of the compensator significantly improves the performance. Compared to the servo positioning example, the tracking performance for low-velocity references is less smooth, due to a higher noise level of the angle sensor.

VIII. Conclusion

In this work, an adaptive friction compensation technique is proposed and analyzed. In the proposed method, the friction force is computed as the product of a time-varying friction parameter and a signum function. A realistic definition of the signum function for the purpose of friction modeling is specified. As this definition of the signum function depends, besides on the velocity and control input, on the value of the friction, which is unknown, it is not useful for compensation purpose. Therefore, an estimate of this signum function is derived for the use in the compensation scheme. The resulting closed-loop system is analyzed and global asymptotic stability of the position and velocity errors is proven. An important property of the compensator is that if the system is in standstill and the position and velocity errors are zero, the compensator automatically switches off. However, this compensator keeps on adapting when there is an offset, even if the system is in standstill. Simulations and experimental results show the tracking performance improvement achieved by the compensator. The undesired effects of friction are almost completely eliminated: steady-state errors disappear and the stick-slip behavior is considerably reduced. Even if the friction force is extremely high or rapidly varying, the compensation scheme is capable of eliminating the undesired friction behavior.

A positive feature of the proposed method is that it can compensate a wide range of friction behaviors reasonably well, without requiring detailed friction modeling. Because of this, the compensation method can be easily implemented in various systems, like a servo motor or a robotic manipulator, all of which are subjected to different friction behaviors. As k_c is updated based on feedback control, problems may occur for rapidly varying friction forces. However, except around velocity reversals, the friction variation over time is fairly

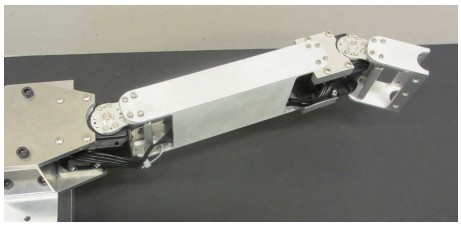

Fig. 10: 2-DOF manipulator.

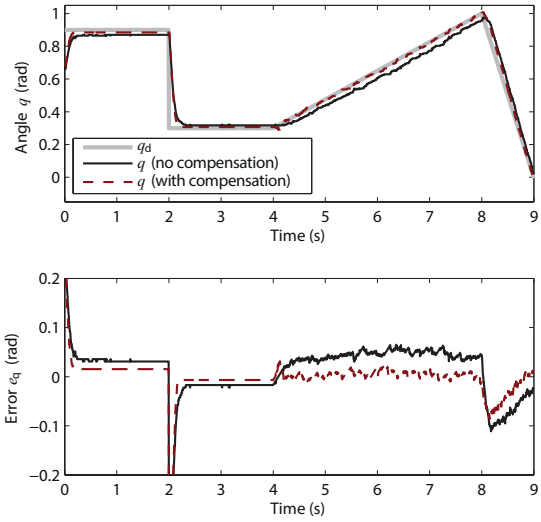

Fig. 11: Tracking performance for the distal link of the 2-DOF robot arm ($\lambda = 10$, $P = 0.2$).

[3]The control signal to the Dynamixel servo is normalized to the range $[-1,\ 1]$. The exact voltage applied to the motor is unknown.

gradual. As the abrupt variations around zero velocity are captured by the sign change of the signum function and the other variations can be accommodated by a proper tuning of the parameter P, in most situations, the feedback control will not lead to real problems. A limitation of the proposed scheme is that it is friction-specific and cannot deal with disturbances that do not always oppose motion. These can, however, be compensated by other techniques. Another possible room for improvement is in the low-velocity range, where stick-slip motion occurs at very high fiction levels.

REFERENCES

[1] B. Bona and M. Indri, "Friction compensation in robotics: an overview," in Proc. of the 44th IEEE Conf. on Decision and Control, Seville, Spain, 2005, pp. 4360 – 4367.

[2] B. Friedland and Y. Park, "On adaptive friction compensation," IEEE Trans. on Automatic Control, vol. 37, no. 10, pp. 1609 –1612, 1992.

[3] B. Friedland and S. Mentzelopoulou, "On adaptive friction compensation without velocity measurement," in Proc. of the IEEE Conf. on Control Applications, vol. 2, Dayton, OH, USA, 1992, pp. 1076 –1081.

[4] A. Yazdizadeh and K. Khorasani, "Adaptive friction compensation based on the Lyapunov scheme," in Proc. of the IEEE Int. Conf. on Control Applications, Dearborn, MI, USA, 1996, pp. 1060 –1065.

[5] T. Liao and T. Chien, "An exponentially stable adaptive friction compensator," IEEE Trans. on Automatic Control, vol. 45, no. 5, pp. 1076–1081, 2000.

[6] T. Zhang and M. Guay, "Comments on "An exponentially stable adaptive friction compensator"," IEEE Trans. on Automatic Control, vol. 46, no. 11, pp. 1844–1845, 2001.

[7] Y. Zhu and P. Pagilla, "Static and dynamic friction compensation in trajectory tracking control of robots," in Proc. of the IEEE Int. Conf. on Robotics and Automation, Washington DC, USA, 2002, pp. 2644 – 2649.

[8] H. Ahn and Y. Chen, "Time periodical adaptive friction compensation," in Proc. of the IEEE Int. Conf. on Robotics and Biomimetics, Shenyang, China, 2004, pp. 362 –367.

[9] ——, "State periodic adaptive friction compensation," in Proc. of the 16th IFAC World Congress, Prague, Czech Republic, 2005.

[10] M. Noorbakhsh and A. Yazdizadeh, "Adaptive friction compensation in a two-link planar robot manipulator using a new Lyapunov-based controller," in Proc. of the 8th IEEE Int. Conf. on Control and Automation, Xiamen, China, 2010, pp. 2132 –2137.

[11] C. Canudas de Wit and P. Lischinsky, "Adaptive friction compensation with partially known dynamic friction model," Int. Journal of Adaptive Control and Signal Processing, vol. 11, no. 3, pp. 65–80, 1997.

[12] S. Susanto, R. Babuška, F. Liefhebber, and T. van der Weiden, "Adaptive friction compensation: Application to a robotic manipulator," in Proc. of the 17th IFAC World Congress, Seoul, Korea, 2008, pp. 2020–2024.

[13] L. Freidovich, A. Robertsson, A. Shriaev, and R. Johansson, "LuGre-model based friction compensation," IEEE Trans. on Control Systems Technology, vol. 18, no. 1, pp. 194–200, 2010.

[14] J. Yen, S. Huang, and S. Lu, "A new compensator for servo systems with position dependent friction," Journal of Dynamic Systems, Measurent and Control, vol. 112, pp. 612–618, 1999.

[15] K. Worden, C. Wong, U. Parlitz, A. Hornstein, D. Engster, T. Tjahjowido, F. Al-Bender, D. Rizos, and S. Fassois, "Identification of presliding and sliding friction dynamics: grey box and black-box models," Mechanical Systems and Signal Processing, vol. 21, no. 1, pp. 514–534, 2007.

[16] H. Wang, C. Vasseur, and V. Koncar, "Friction compensation of an X-Y robot using a recursive model free controller," in IEEE Int. Conf. on Industrial Technology, Vina del Mar, Chile, 2010, pp. 355 –360.

[17] X. Gao and S. Ovaska, "Friction compensation in servo motor systems using neural networks," in Proc. of the 1999 IEEE Midnight-Sun Workshop on Soft Computing Methods in Industrial Applications, 1999, pp. 146 –151.

[18] T. H. Lee, K. K. Tan, and S. Huang, "Adaptive friction compensation with a dynamical friction model," Mechatronics, IEEE/ASME Trans. on, vol. 16, no. 1, pp. 133–140, Feb 2011.

[19] H. Chaoui and P. Sicard, "Adaptive friction compensation of flexible-joint manipulators with parametric uncertainties," in IEEE Int. Conf. on Automation Science and Engineering, Madison, WI, 2013, pp. 300–305.

[20] A. Conceicao, A. Moreira, and P. Costa, "Practical approach of modeling and parameters estimation for omnidirectional mobile robots," IEEE/ASME Trans. on Mechatronics, vol. 14, no. 3, pp. 377–381, June 2009.

[21] J. Lins Barreto S, A. Scolari Conceicao, C. Dorea, L. Martinez, and E. De Pieri, "Design and implementation of model-predictive control with friction compensation on an omnidirectional mobile robot," IEEE/ASME Trans. on Mechatronics,, vol. 19, no. 2, pp. 467–476, April 2014.

[22] J. Ryu, J. Song, and D. Kwon, "A nonlinear friction compensation method using adaptive control and its practical application to an in-parallel actuated 6-DOF manipulator," Control Engineering Practice, vol. 9, no. 2, pp. 159 – 167, 2001.

[23] W. Rugh, Linear system theory. Prentice Hall, 1993.

[24] R. Shorten, F. Wirth, O. Mason, K. Wulff, and C. King, "Stability criteria for switched and hybrid systems," SIAM review, vol. 49, no. 4, pp. 545–592, 2007.

[25] G. Michaletzky and L. Gerencsér, "BIBO stability of linear switching systems," IEEE Trans. on Automatic Control, vol. 47, no. 11, pp. 1895–1898, 2002.

[26] A. N. Michel and L. Hou, "Stability results involving time-averaged lyapunov function derivatives," Nonlinear Analysis: Hybrid Systems, vol. 3, no. 1, pp. 51–64, 2009.

[27] K. Åström and B. Wittenmark, Computer controlled systems. Prentice Hall, 1997.

K. Verbert received the B.Eng. degree (cum laude) in Human Kinetic Technology from the Hague University of Applied Sciences, The Hague, The Netherlands, in 2009 and the M.Sc. degree (cum laude) in Control Engineering from the Delft University of Technology, Delft, The Netherlands, in 2012. She is currently working towards the Ph.D. degree at the Delft Center for Systems and Control, Delft University of Technology. Her current research interests include fault diagnosis, maintenance optimization, friction compensation, and (human) motion control.

R. Tóth received the B.Sc. degree in electrical engineering and the M.Sc. degree in information technology in parallel at the University of Pannonia, Veszprém, Hungary, in 2004, and the Ph.D. degree (cum laude) from the Delft Center for Systems and Control (DCSC), Delft University of Technology (TUDelft), Delft, The Netherlands, in 2008. He was a Post-Doctoral Research Fellow at DCSC, TUDelft, in 2009 and at the Berkeley Center for Control and Identification, University of California, Berkeley, in 2010. He held a position at DCSC, TUDelft, in 2011-12. Currently, he is an Assistant Professor at the Control Systems Group, Eindhoven University of Technology (TU/e). He is an Associate Editor of the IEEE Conference Editorial Board. His research interest is in linear parameter-varying (LPV) and nonlinear system identification, machine learning, process modeling and control, and behavioral system theory. Dr. Tóth received the TUDelft Young Researcher Fellowship Award in 2010.

R. Babuška received the M.Sc. degree (cum laude) in control engineering from the Czech Technical University in Prague, in 1990, and the Ph.D. degree (cum laude) from the Delft University of Technology, the Netherlands, in 1997. He has had faculty appointments at the Technical Cybernetics Department of the Czech Technical University Prague and at the Electrical Engineering Faculty of the Delft University of Technology. Currently, he is a Professor of Intelligent Control and Robotics at the Delft Center for Systems and Control. His research interests include reinforcement learning, neural and fuzzy systems, identification and state-estimation, nonlinear model-based and adaptive control and dynamic multi-agent systems. He has been working on applications of these techniques in the fields of robotics, mechatronics, and aerospace.